

Single-Channel Properties of a Volume-sensitive Anion Conductance

Current Activation Occurs by Abrupt Switching of Closed Channels to an Open State

PAUL S. JACKSON* and KEVIN STRANGE†

From the Critical Care Research Laboratories, Departments of *Neurosurgery and †Medicine (Nephrology), Children's Hospital and Harvard Medical School, Boston, Massachusetts 02115

ABSTRACT Swelling-induced loss of organic osmolytes from cells is mediated by an outwardly rectified, volume-sensitive anion channel termed VSOAC (Volume-Sensitive Organic osmolyte/Anion Channel). Similar swelling-activated anion channels have been described in numerous cell types. The unitary conductance and gating kinetics of VSOAC have been uncertain, however. Stationary noise analysis and single-channel measurements have produced estimates for the unitary conductance of swelling-activated, outwardly rectified anion channels that vary by >15-fold. We used a combination of stationary and nonstationary noise analyses and single-channel measurements to estimate the unitary properties of VSOAC. Current noise was analyzed initially by assuming that graded changes in macroscopic current were due to graded changes in channel open probability. Stationary noise analysis predicts that the unitary conductance of VSOAC is ~1 pS at 0 mV. In sharp contrast, nonstationary noise analysis demonstrates that VSOAC is a 40–50 pS channel at +120 mV (~15 pS at 0 mV). Measurement of single-channel events in whole-cell currents and outside-out membrane patches confirmed the nonstationary noise analysis results. The discrepancy between stationary and nonstationary noise analyses and single-channel measurements indicates that swelling-induced current activation is not mediated by a graded increase in channel open probability as assumed initially. Instead, activation of VSOAC appears to involve an abrupt switching of single channels from an OFF state, where channel open probability is zero, to an ON state, where open probability is near unity.

INTRODUCTION

Maintenance of a constant volume in the face of extracellular and intracellular osmotic perturbations is a critical problem faced by all animal cells. Cells respond to volume changes by activating volume regulatory mechanisms that mediate the net gain or loss of osmotically active solutes. Both inorganic ions (Hallows and Knauf,

Address correspondence to Dr. Kevin Strange, Children's Hospital, Enders 12, 300 Longwood Avenue, Boston, MA 02115.

1994) as well as small organic solutes (amino acids, polyols, and methylamines) termed organic osmolytes (Garcia-Perez and Burg, 1991; Yancey, 1994) are used by cells for volume control.

Loss of organic osmolytes from cells is brought about by rapid (i.e., seconds) increases in passive efflux via a swelling-activated anion-selective channel (e.g., Banderali and Roy, 1992; Kirk, Ellory, and Young, 1992; Jackson and Strange, 1993; Jackson, Morrison, and Strange, 1994; reviewed by Strange and Jackson, 1995). In rat C6 glioma cells, this channel is outwardly rectified, has a broad anion selectivity ($\text{SCN}^- > \text{I}^- > \text{NO}_3^- > \text{Br}^- > \text{Cl}^- > \text{F}^- > \text{isethionate} > \text{gluconate}$) and is inactivated by membrane voltages above +60 mV (Jackson and Strange, 1993; see Jackson and Strange, 1995). Swelling-induced channel activation has an absolute requirement for intracellular nonhydrolytic ATP binding (Jackson et al., 1994) and may be modulated by intracellular Cl^- and/or ionic strength (Strange, 1994; Strange, Churchwell, Ballatori, Boyer, and Jackson, 1995). Because cells possess several different types of volume-sensitive anion channels that may have different volume regulatory functions (reviewed by Strange, 1994; Strange and Jackson, 1995), we have termed the channel responsible for organic osmolyte efflux VSOAC (Volume-Sensitive Organic osmolyte/Anion Channel). Swelling-activated whole-cell anion conductances similar to VSOAC have been described in numerous mammalian cell types (reviewed by Strange and Jackson, 1995), *Xenopus* oocytes (Ackerman, Wickman, and Clapham, 1994), and recently, in hepatocytes of the skate *Raja erinacea* (Strange et al., 1995).

The single-channel properties of VSOAC are poorly understood despite its widespread occurrence and essential physiological role. Stationary noise analysis studies have suggested that the channel responsible for swelling-activated whole-cell anion conductance in chromaffin cells (Doroshenko and Neher, 1992), neutrophils (Stoddard, Steinbach, and Simchowicz, 1993), T cells (Lewis, Ross, and Cahalan, 1993) and human endothelial cells (Nilius, Oike, Zahradnik, and Droogmans, 1994) is very small ($\leq 1\text{--}2$ pS at 0 mV). Single-channel measurements in epithelial cells have demonstrated the existence of a swelling-induced, outwardly rectified anion channel with a unitary conductance of 40–90 pS at strongly depolarizing voltages (Worrell, Butt, Cliff, and Frizzell, 1989; Solc and Wine, 1991; Okada, Petersen, Kubo, Morishima, and Tominaga, 1994). In the present study we utilized stationary and nonstationary noise analyses and single-channel measurements to determine the unitary properties of VSOAC. Noise analysis was performed initially by making the conventional assumption that graded changes in macroscopic current were due to graded changes in channel open probability. Our results demonstrate that stationary noise analysis underestimates the unitary conductance of VSOAC by ~15-fold. We conclude that current activation is not mediated by a graded increase in channel open probability as generally assumed. Instead, increases in whole-cell anion current appear to be due to an increase in the number of active channels in the cell membrane.

MATERIALS AND METHODS

Cell Culture

Rat C6 glioma cells were cultured in Eagle's minimal essential medium (MEM; Gibco Laboratories, Gaithersburg, MD) with 10% fetal bovine serum (FBS) and penicillin/streptomycin.

cin as described previously (Jackson and Strange, 1993). The osmolality of the growth medium was elevated 24–48 h before the cells were used by adding NaCl directly to the MEM. The osmolalities of the normal and hypertonic growth media were measured using a freezing point osmometer (model Osmette A, Precision Instruments, Sudbury, MA) and were 295–300 mosmol/kg H₂O (mOsm) and 385–390 mOsm, respectively.

Patch Clamp Recordings

C6 glioma cells were grown on 12-mm diam glass cover slips, acclimated to 390 mOsm MEM for 24–48 h, and patch clamped in the whole-cell configuration at room temperature with symmetrical CsCl solutions as described previously (Jackson and Strange, 1993). Patch electrodes were pulled from 1.5 mm o.d. borosilicate glass microhematocrit tubes (Fisher Scientific, St. Louis, MO) that had been silanized with dimethyl-dichloro silane (Sigma Chemical Co., St. Louis, MO). The electrodes were not fire polished before use and had DC resistances of 3–5 M Ω . Cells were used only if the series resistance was < 10 M Ω .

An Axopatch 200A (Axon Instruments, Inc., Foster City, CA) patch clamp amplifier was used to voltage clamp C6 cells after gigaseal formation and attainment of whole-cell access. Command voltage generation, data digitization and data analysis were carried out on an 80486, 100 MHz IBM-compatible computer (Dell Optiplex 4100/MX, Austin, TX) using a DigiData 1200 AD/DA interface with pClamp software (Axon Instruments, Inc.). Electrical connections to the amplifier were made using Ag/AgCl pellets and 3 M KCl/agar bridges. Series resistance compensation of 70% was used for whole-cell recordings.

Solutions

Cells were patch clamped with a pipette solution containing 140 mM CsCl, 2 mM MgSO₄, 20 mM HEPES, 6 mM CsOH, 1 mM EGTA, 0.5 mM GTP, 2 mM ATP and 50 mM raffinose (pH = 7.2; osmolality = 365–375 mOsm). The control bath solution contained 140 mM CsCl, 5 mM MgSO₄, 12 mM HEPES, 8 mM TRIS and 80 mM raffinose (pH = 7.4; osmolality = 385–390 mOsm). Cell swelling was induced by removing raffinose to reduce bath osmolality to 300 mOsm.

Stationary Noise Analysis

Swelling-activated currents were recorded on video tape using an Instrutech model VR-10B digital data recorder (Instrutech Corp., Great Neck, NY) and a Sony SLV-400 VHS video cassette recorder (Sony Corporation of America, Park Ridge, NJ). Recorded data were played back through an 8-pole Bessel filter (Frequency Devices Inc., Haverhill, MA) at 2 kHz and digitized at 5–10 kHz. Current records 100–250 ms long were digitized every 5 s throughout the time course of swelling-induced current activation. Mean current and variance were computed for each record using pClamp software (Axon Instruments, Inc.). The baseline variance before activation of the current was subtracted from all of the data points.

Spectral Analysis

Whole-cell current recordings for spectral analysis were filtered at 5 kHz with an 8 pole Bessel filter and digitized at 20 kHz. Current recordings were collected before induction of cell swelling (preswelling) and 2–9 min after reduction of bath osmolality (postswelling). For each power spectrum, a total of 64 current records 50–125 ms long were collected, Fourier transformed using Origin software (Microcal Software, Inc., Northampton, MA) and averaged. The preswelling baseline power spectrum was subtracted from the postswelling power spectrum to yield the spectral density of the noise associated with current activation.

Nonstationary Noise Analysis

Nonstationary noise analyses was carried out on whole-cell currents during depolarization-induced inactivation (e.g., Sigworth, 1980; Conti, Hille, and Nonner, 1984; Heinemann and Conti, 1992). Membrane potential was held at -60 or -80 mV. After attainment of stable swelling-induced current levels, channel inactivation was initiated by voltage pulses (0.5–4 s long) to depolarizing membrane potentials ($+100$ to $+160$ mV). Current inactivation recordings were filtered with an 8-pole Bessel filter at 0.5 kHz or 5 kHz and digitized at 1 or 10 kHz. The inactivation protocol was repeated on individual cells 47–350 times and a mean current and variance were calculated at each time point. Variance was computed by the method of successive differences (Heinemann and Conti, 1992) using custom software written in BASIC. Variance data were binned into 50-pA bins so that equal weight was given to each current level during the fitting procedure (Heinemann and Conti, 1992).

Calculation of Unitary Currents and Chord Conductances

Because VSOAC is outwardly rectified, it is necessary to use a conversion procedure when comparing single-channel conductance levels at different voltages. Expected single-channel currents and chord conductances were calculated by scaling the whole-cell current-to-voltage curve (see Fig. 6A in the following paper, Jackson and Strange, 1995) to the single-channel data and measuring its slope and amplitude at the desired voltage.

RESULTS

Single-Channel Conductance Estimated by Stationary Noise Analysis

As described in the following paper (Jackson and Strange, 1995), activation of VSOAC accounts for $\geq 90\%$ of the whole-cell anion current induced by swelling in C6 glioma cells. To estimate the single-channel conductance of VSOAC, we performed stationary noise analysis on whole-cell Cl^- currents at various times after swelling-induced current activation. This approach is based on the following assumptions: (a) there are N independent and identical channels in the membrane; and (b) the channels have two conductance states, open and closed, that obey binomial statistics. It follows from these assumptions that the mean whole-cell current I , is related to the single-channel properties as

$$I = NiP_o \quad (1)$$

where i is the single-channel current and P_o is the channel open probability. Current variance σ^2 then, is related to the single-channel properties as

$$\sigma^2 = iI - I^2/N. \quad (2)$$

Eq. 2 can be used to determine i and N if I and σ^2 are determined for various channel open probabilities. Calculation of i and N during graded current activation from Eq. 2 assumes that (a) activation of the current is a consequence of a graded increase in the open probability of all the channels; (b) the single-channel conductance does not change during activation; and (c) the number of channels contributing to the variance remains constant during activation.

Fig. 1A shows the Cl^- current activated by swelling in a single C6 glioma cell. The swelling-induced current increased at a rate of 1 pA/s. Current variance was

determined by digitizing currents for 100-ms sampling periods at various times after activation (Fig. 1 *B*). The whole-cell current changed insignificantly over this sampling period compared to the current variance.

A plot of variance versus current is shown for this cell in Fig. 1 *C*. The data were fit using Eq. 2. The single-channel current at the holding potential of -50 mV estimated from this plot was -0.037 pA and N was 58,734. This single-channel current corresponds to a unitary chord conductance, γ , of 0.55 pS at -50 mV and 1.2 pS at 0 mV estimated from the measured whole-cell current-to-voltage relationship. The mean \pm SE i , N and γ were -0.038 ± 0.007 pA at -50 mV; $68,670 \pm 17,296$ (range 12,936–136,390) and 0.55 ± 0.09 pS at -50 mV and 1.2 ± 0.2 pS at 0 mV ($n = 6$), respectively.

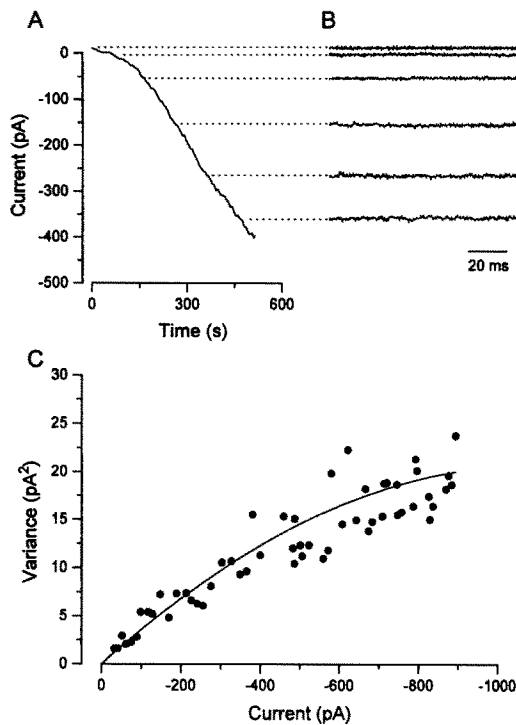


FIGURE 1. Estimation of unitary conductance of VSOAC by stationary noise analysis. (*A*) Swelling-induced Cl^- current activation in a single C6 glioma cell. Holding potential was -50 mV. (*B*) Examples of 100-ms current records used for determination of current variance. Dashed lines connected to *A* indicate the times when the samples were digitized during activation of VSOAC. Currents were filtered at 2 kHz and digitized at 5 kHz. (*C*) Current variance plotted as a function of whole-cell current. The solid line was fit to the data using Eq. 2 by nonlinear regression analysis. For this cell, $i = -0.037$ pA, $N = 58,734$ and $\gamma = 0.55$ pS at -50 mV and 1.2 pS at 0 mV.

Fig. 2 *A* shows the spectral analysis of the current noise before and after swelling-induced activation of VSOAC. The difference between these two power spectra is the spectral density of the noise associated with VSOAC activation (Fig. 2 *B*). Data in Fig. 2 *B* were fit with a single Lorentzian described by Eq. 3:

$$S(f) = S(0)/[1 + (f/f_c)^2] \quad (3)$$

where $S(f)$ is the spectral density at frequency f , and f_c is the corner frequency or the frequency at which the power is half maximal. The corner frequency for this curve was 594 Hz. The mean \pm SE corner frequency was 526 ± 49 Hz ($n = 4$). These

results demonstrate that the recording bandwidth of 2 kHz was sufficient to capture accurately the current variance associated with activation of VSOAC.

Single-Channel Conductance Estimated by Nonstationary Noise Analysis

An independent measure of the single-channel properties of VSOAC can be derived from nonstationary noise analysis of whole-cell currents. Nonstationary noise analysis relies on the same assumptions and statistical treatment as described above for stationary noise analysis. Unlike stationary noise analysis, however, this approach measures mean current and variance throughout experimentally-induced transient changes in channel gating. Changes in channel gating are typically induced by

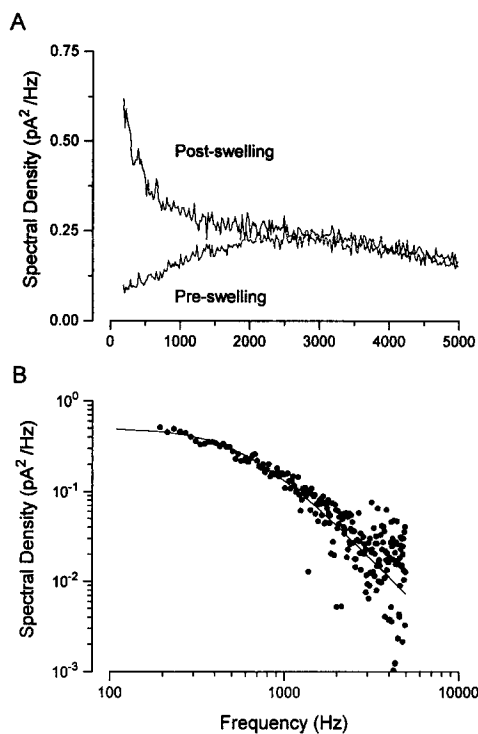


FIGURE 2. Spectral analysis of whole-cell current noise. (A) Spectral analysis of whole-cell current noise before and after swelling-induced activation of VSOAC in a single C6 glioma cell. For each trace, 64 current records lasting 50 ms each were collected, filtered at 5 kHz, digitized at 20 kHz, Fourier transformed and averaged. The postswelling current samples were collected ~2 min after induction of cell swelling. (B) Spectral analysis of current noise due to VSOAC activation. The preswelling spectral analysis was subtracted from the postswelling spectral analysis shown in A. A single Lorentzian was fit to the data by nonlinear regression analysis and is shown by the solid line. The corner frequency f_c for this trace was 594 Hz.

voltage steps (e.g., Sigworth, 1980). After acquiring multiple records of the transient, voltage-induced current response, the individual records are averaged to yield an ensemble average and mean I and σ^2 are determined. The unitary current and number of channels are then estimated using Eq. 2.

Fig. 3 shows an example of an experiment in which nonstationary noise analysis was used to estimate the unitary conductance of VSOAC. As shown in the following paper (Jackson and Strange, 1995), whole-cell swelling-activated anion current is inactivated ~90% in response to strong membrane depolarization. After attainment of a stable swelling-induced current, the cell shown in Fig. 3 was held at -60 mV and then stepped to $+120$ mV for 390 ms. The cell was allowed to recover at -60 mV for

5 s and the voltage step procedure repeated (Fig. 3A). For this cell, 350 current inactivation records were averaged to yield an ensemble average (Fig. 3B) and σ^2 was calculated at each time point (Fig. 3C) using the technique of successive differences (Heinemann and Conti, 1992). Current variance was minimal at the peak current amplitude. As inactivation increased, σ^2 increased and reached a maximum when $\sim 50\%$ of the whole-cell current had been inactivated. The current variance then decreased and reached a minimal value after channel inactivation was complete (Fig. 3C).

Current variance is plotted as a function of the mean current in Fig. 4 and the data were fit using Eq. 2. The single-channel current at the test voltage of +120 mV

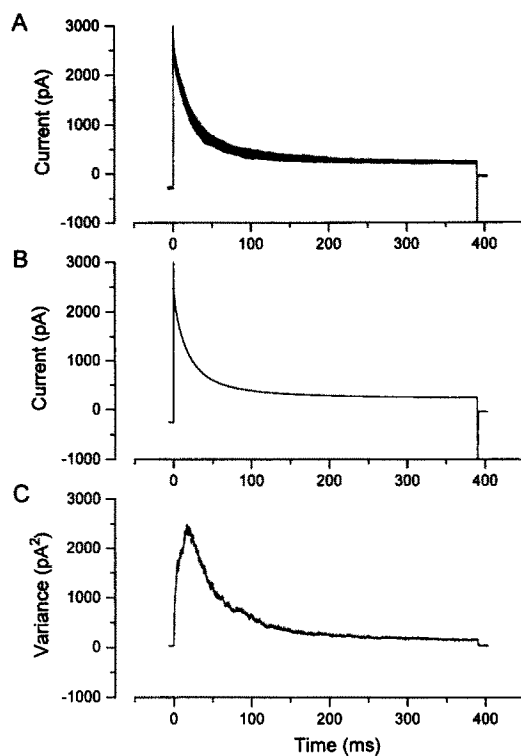


FIGURE 3. Calculation of mean current and variance from voltage-dependent inactivation of VSOAC current. (A) Membrane potential was held at -60 mV and stepped to $+120$ mV for 390 ms once every 5 s. During this time, whole-cell current is inactivated by $\sim 90\%$ (see Jackson and Strange, 1995). This inactivation procedure was repeated 350 times. Figure shows 25 of the 350 current inactivation records collected on this cell. Current records were filtered at 5 kHz and digitized at 10 kHz. (B) Ensemble average of 350 current inactivation records. (C) Current variance determined by the method of successive differences (Heinemann and Conti, 1992). Spikes in the current variance due to capacitive transients were removed from the figure for clarity.

estimated from this plot was 3.0 pA and N was 843. This single-channel current corresponds to a unitary chord conductance of 39.2 pS at +120 mV and 10.8 pS at 0 mV estimated from the measured whole-cell current-to-voltage relationship. Table I shows the results of five separate experiments using test voltages of +100, +120, or +160 mV. The mean \pm SE N and γ were $1,256 \pm 261$ and 50.6 ± 1 pS at +120 mV and 13.1 ± 1.6 pS at 0 mV ($n = 5$), respectively.

Single-Channel Measurements of VSOAC

The difference in the single-channel conductance estimated from the stationary and nonstationary noise analyses was dramatic. To resolve the discrepancy between these

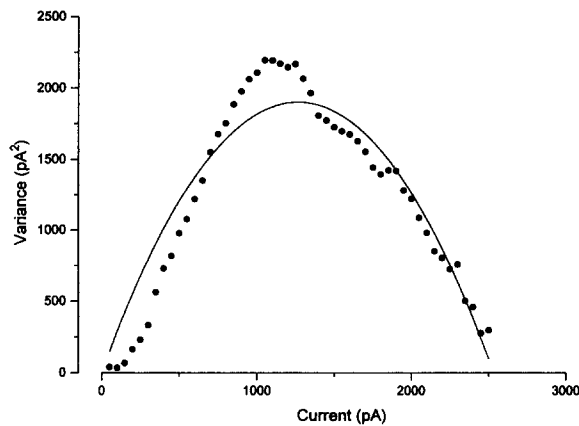


FIGURE 4. Estimation of unitary conductance of VSOAC from nonstationary noise analysis data. The ensemble variance in Fig. 3 was plotted as a function of the mean current. The solid line was fit to the data using Eq. 2 by nonlinear regression analysis. For this cell, $i = 3.0$ pA, $N = 843$ and $\gamma = 39.2$ pS at +120 mV and 10.8 pS at 0 mV.

measurements, we searched for single-channel events in isolated membrane patches. Outside-out patches were pulled from cells after near maximal activation of VSOAC. Membrane patch currents with pharmacological and voltage-dependent characteristics identical to those of VSOAC whole-cell currents were observed regularly. Fig. 5 shows examples of these currents. The current-to-voltage relationship for these patches was outwardly rectified. In addition, the currents exhibited voltage-independent inhibition by 100 μ M ketoconazole (Jackson and Strange, 1993; McManus, Serhan, Jackson, and Strange, 1994) and voltage-dependent block by 10 mM ATP (Jackson and Strange, 1995).

Membrane patch currents also exhibited depolarization-induced inactivation (Fig. 6). The mean \pm SE τ for inactivation at +120 mV was 261 ± 46 ms ($n =$ six patches), similar to that seen in the whole cell (264 ± 25 ms; Jackson and Strange, 1995). Unlike the whole-cell current, however, current inactivation in the isolated patches occurred in discrete steps (Figs. 6 and 8). Fig. 7 shows a plot of single-channel current at various test voltages determined from these step closures. The slope

TABLE I
Estimates of i , N , and γ Derived from Nonstationary Noise Analysis of VSOAC
Current During Depolarization-induced Inactivation

Test voltage	Unitary current	Number of channels	Estimated unitary chord conductance at test voltage	Estimated unitary chord conductance at 0 mV
mV	pA		pS	pS
+160	8.9	790	89.5	18.9
+120	3.8	2,156	49.7	13.1
+120	3.0	843	39.2	10.2
+120	3.7	951	48.8	12.7
+100	2.4	1,540	39.2	10.8

Table shows the results obtained from five separate cells where VSOAC current was inactivated by voltage steps of +100, +120, or +160 mV. The chord conductance was calculated at the test voltage and at 0 mV from the measured whole cell current-to-voltage relationship.

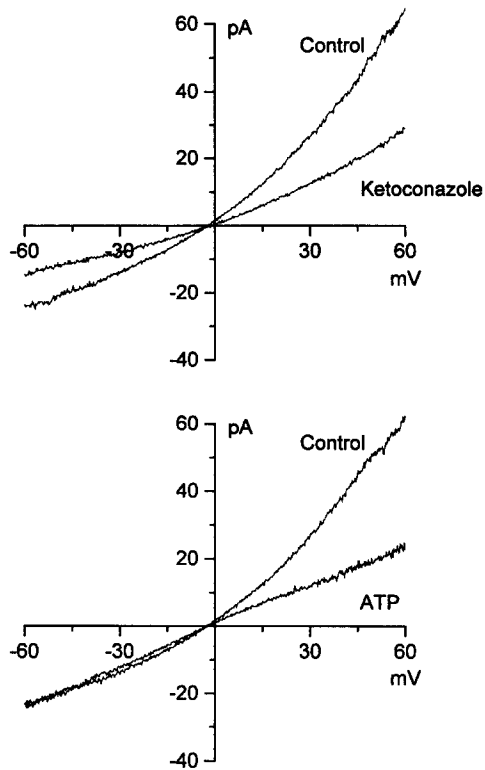


FIGURE 5. Current-to-voltage relationship in outside-out membrane patches pulled from swollen C6 cells. Membrane potential was ramped from -60 to $+60$ mV at 60 mV/s. Control currents are outwardly rectified. Extracellular application of 100 μ M ketoconazole blocked the current in a voltage-independent manner. Exposure of patches to 10 mM Na_2ATP produced a voltage-dependent current block. The effects of both agents were fully reversible (data not shown). Ketoconazole was added to the bathing medium as a stock solution dissolved in DMSO. The final DMSO concentration was 0.1% , which has no effect on channel activity (Jackson and Strange, 1993; McManus et al., 1994).

conductance estimated from this plot was 57.2 pS. Using the mean \pm SE single-channel current of 5.1 ± 0.09 pA ($n = 162$ single-channel closures; 18 patches) measured at $+120$ mV, the chord conductance estimated from the whole-cell current-to-voltage relationship was 66.7 ± 1.2 pS. These values are in close

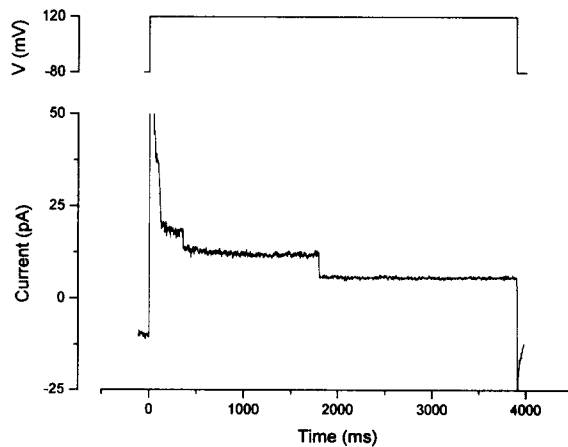


FIGURE 6. Membrane patch currents display depolarization-induced inactivation. The patch was pulled in the outside-out configuration from a swollen C6 cell. Patch current displayed an outwardly rectified current-to-voltage relationship. Recordings were filtered at 0.5 kHz and digitized at 1 kHz. Inactivation occurred in discrete steps. The mean step size in this patch was 5.4 pA at $+120$ mV. Multiple voltage steps (data not shown) revealed that the patch contained seven channels.

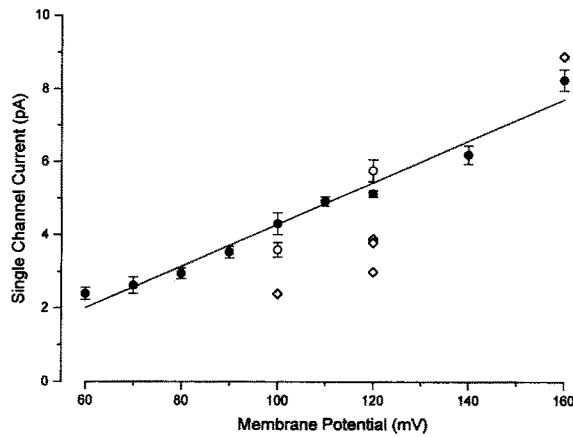


FIGURE 7. Plot of single-channel current vs membrane potential. Patches were pulled from swollen cells in the outside-out configuration and held at -60 or -80 mV. Channel inactivation was elicited by depolarizing voltage steps. Solid points represent the means \pm SE of the single-channel currents determined from 3–162 channel closures observed in 1–18 membrane patches. (Solid line) Fit to the data using linear regression analysis ($y = -1.4$

$\text{pA} + 0.0572 \text{ pA/mV}$; $r = 0.99$). (Open diamonds) Single-channel currents determined from nonstationary noise analysis (Table I). (Open circles) The means \pm SE of single-channel events observed in whole-cell recordings (Fig. 10).

agreement with the chord conductance of 51 pS at $+120$ mV estimated from nonstationary noise analysis (Fig. 6).

Occasionally, during inactivation experiments, rapid, transient single-channel closures could be observed before complete channel inactivation. Fig. 8 shows an extreme example of this behavior (cf. Fig. 6). For the 6 s of recording time during which there was only one channel open in this patch, we estimated a single-channel P_o of 0.975. A total of 35 s of recordings during periods in which only a single channel was open were obtained on eight separate patches. The mean estimated P_o for these patches was 0.99.

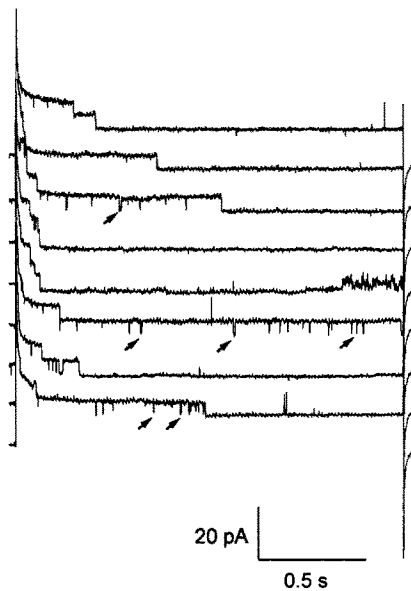


FIGURE 8. Single-channel records obtained from an outside-out patch illustrating transient closures (arrowheads) observed during depolarization-induced inactivation. Patch was held -60 mV and stepped to $+120$ mV for 2 s every 10 s. Records were filtered at 0.5 kHz and digitized at 2 kHz.

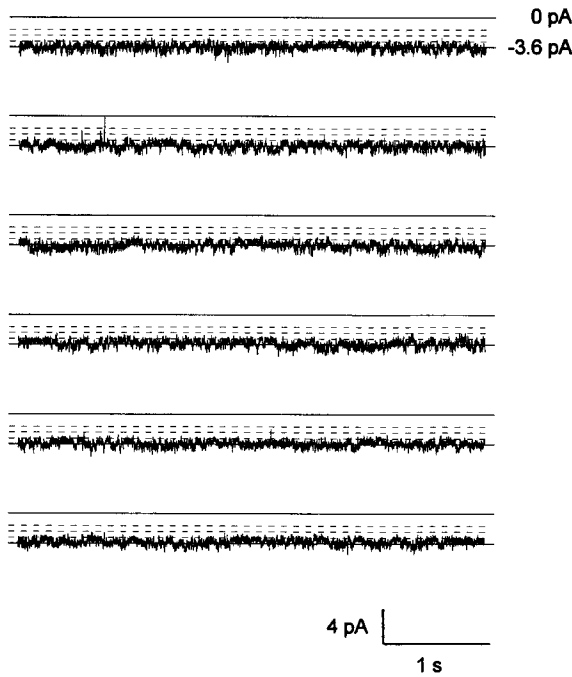


FIGURE 9. Current record from an outside-out patch held at -80 mV. Depolarization-induced inactivation revealed that this patch contained three channels. The dashed lines denote current steps that should be observed for the closing of one, two or three of these channels. Current steps were calculated using $i = -0.7$ pA as determined from single-channel measurements (see Results).

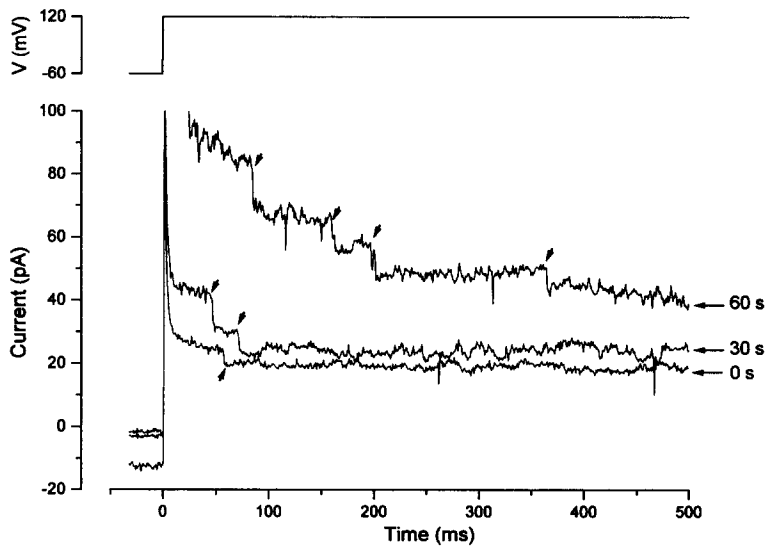


FIGURE 10. Single-channel events (*arrowheads*) observed in whole-cell recordings. Cell was held at -60 mV and stepped to $+120$ mV for 500 ms. Inactivation recordings were obtained immediately after (i.e., 0 s) and 30 and 60 s after reduction of bath osmolality. Recordings were filtered at 0.5 kHz and digitized at 2 kHz. The mean unitary current observed in this cell during depolarization-induced inactivation was 5.8 pA.

When patches were held at negative voltages, distinct single-channel events were not observed. A sample 30-s recording from a patch held at -80 mV is shown in Fig. 9. Depolarization-induced inactivation revealed that this patch contained three channels (data not shown). The dashed lines indicate the expected current levels for closure of one, two or three of these channels. We conclude from these results that the open probability of VSOAC is close to unity when the channel is activated by cell swelling.

Measurement of Single-Channel Events in Whole-Cell Currents

Single-channel events could also be observed during depolarization-induced inactivation of whole-cell currents. An example of this is shown in Fig. 10. For these measurements, it was essential to use cells that had very low resting anion and nonspecific leak currents. It was also essential to carry out the measurements in the very early stages of swelling-induced current activation so that amplifier gain could be maximized and resolution of single-channel closures made possible. The mean \pm SE single-channel currents measured in two separate cells depolarized to $+100$ or $+120$ mV were 3.6 ± 0.2 pA ($n =$ five single-channel events) and 5.8 ± 0.3 pA ($n =$ seven single-channel events), respectively. As shown in Fig. 6, these values are in close agreement with those obtained by nonstationary noise analysis and in outside-out patch recordings.

Loss of Channel Activity from Membrane Patches

Single channels were rarely observed in isolated patches. Instead, we typically found that patches contained at least three to four channels (e.g., Figs. 6 and 8). This suggests the possibility that channels cluster in the cell membrane.

The stability of VSOAC in outside-out patches was low (see also Solc and Wine, 1991). Channels were typically active in patches for periods of time ranging from 30 s to a few minutes. Interestingly, the loss of channel activity from a patch was always abrupt and usually occurred for all channels simultaneously. The mechanism of channel loss is unknown at present, but it could be due to diffusion of the channels into the glass-membrane seal region (e.g., see Wunder and Colombini, 1991). The simultaneous loss of all channels from the patch suggests the possibility of significant channel-channel interaction.

DISCUSSION

Single-Channel Properties of VSOAC: Mini Vs Intermediate Conductance Channels

The unitary properties of VSOAC have been uncertain. Stationary noise analysis yielded an estimated unitary conductance at 0 mV of ~ 1 – 2 pS for the swelling-activated anion channel in chromaffin cells, endothelial cells, neutrophils, and T cells (Doroshenko and Neher, 1992; Stoddard et al., 1993; Lewis et al., 1993; Nilius et al., 1994). In sharp contrast, swelling-activated anion currents in epithelial cells have been attributed to a much larger channel. Single-channel transitions measured in whole-cell currents of T84 cells (Worrell et al., 1989) and in cell-attached and outside-out patches from T84, intestine 407, tracheal, sweat duct, and sweat secretory

coil cells (Solc and Wine, 1991; Okada et al., 1994) have demonstrated the existence of an outwardly rectified anion channel that is inactivated by strong depolarization. Solc and Wine (1991) and Okada et al. (1994) have estimated the P_o of this channel to be close to unity. The unitary conductances estimated from single-channel closures observed at +100 mV in these epithelial cells are ~40–90 pS (Worrell et al., 1989; Solc and Wine, 1991; Okada et al., 1994).

Are different types of channels responsible for the whole-cell currents in different cell types? The swelling-activated whole-cell currents described in these diverse cell types have very similar characteristics with the exception of their voltage-sensitivity. Swelling-activated currents in neutrophils, T cells and endothelial cells show little or no voltage sensitivity, whereas those in epithelial cells are inactivated by strong depolarization. This could suggest that there are two types of outwardly-rectified swelling-activated anion channel. The results described in this paper, however, suggest an alternate possibility. Stationary noise analysis of swelling-activated currents in C6 cells yielded a single-channel conductance of 1.2 pS at 0 mV, a value in close agreement with studies performed on neutrophils, T cells, chromaffin cells and endothelial cells (Doroshenko and Neher, 1992; Stoddard et al., 1993; Lewis et al., 1993; Nilius et al., 1994). The results of current spectral analyses in C6 cells (Fig. 2) and T cells (Lewis et al., 1993) are in similar close agreement. Nonstationary noise analysis and single-channel measurements in whole-cell currents and outside-out patches failed to confirm our stationary noise analysis findings, however. Instead, they demonstrate that the unitary conductance of the channel responsible for the whole-cell current in C6 cells is ~40–50 pS at +120 mV, a result consistent with studies in epithelial cells (Worrell et al., 1989; Solc and Wine, 1991; Okada et al., 1994). We conclude that stationary noise analysis underestimates the unitary conductance of VSOAC by ~15-fold when it is assumed that graded changes in I are brought about by graded changes in P_o .

Validity of Assumptions Underlying Stationary Noise Analysis

Changes in whole-cell currents can be brought about by changes in channel P_o , single-channel current (i) and/or channel number (N). Correct interpretation of whole-cell current noise data therefore requires knowledge of the way in which channel activation occurs. As illustrated by Eq. 2, it is generally assumed that a graded increase in macroscopic current is due to a graded increase in P_o of a constant number of independent channels with a fixed unitary current (e.g., Hille, 1992). Previous stationary noise analysis studies of swelling-activated whole-cell anion currents have been performed under these assumptions (Doroshenko and Neher, 1992; Stoddard et al., 1993; Lewis et al., 1993; Nilius et al., 1994). As demonstrated by the present study, stationary noise analysis substantially underestimates the true unitary conductance of VSOAC. Thus, one or more of these assumptions must be incorrect for the mechanism of swelling-induced channel activation. This conclusion is illustrated by Fig. 11. The upper curve in the figure was derived using Eq. 2. For the calculation of σ^2 , we used a unitary current of -0.43 pA at -50 mV determined by single-channel measurements and the whole-cell current-to-voltage relationship. The number of channels N was 2,100 (see Table I), which was estimated by dividing the maximum whole-cell current observed (-900 pA) by the unitary current of -0.43

pA. The expected variance versus current relationship is dramatically different from the actual data obtained by stationary noise analysis (*solid points*).

Which of the assumptions underlying stationary noise analysis is incorrect? The assumption that single-channel current does not change during activation is valid. We measured unitary currents by nonstationary noise analysis and in outside-out patches. In both sets of measurements, whole-cell current was maximally or near-maximally activated before the measurement was carried out. We also measured single-channel events in whole-cell currents during depolarization-induced inactivation (Fig. 10).

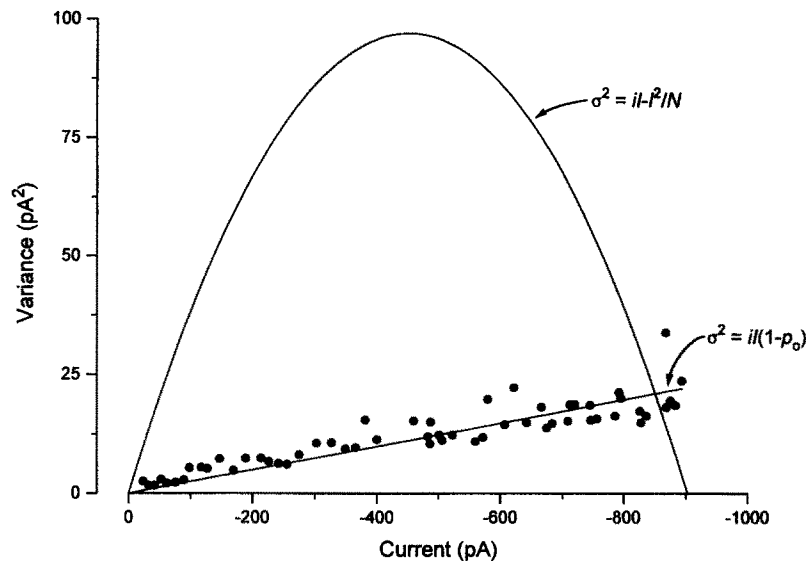
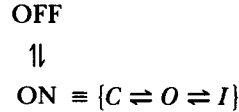


FIGURE 11. Variance vs current relations for different models of VSOAC activation. (*Solid points*) Stationary noise analysis data replotted from Fig. 1 C. The upper curve shows the expected current variance calculated assuming that activation of VSOAC occurs by a graded increase in P_o (Eq. 2). For these calculations, we used a unitary current of -0.43 pA at -50 mV determined by single-channel measurements and the whole-cell current-to-voltage relationship. The number of channels N was 2,100 (see Table I), which was estimated by dividing the maximum whole-cell current observed (-900 pA) by the unitary current of -0.43 pA. (*Lower curve*) Expected variance assuming a variable N and a fixed P_o . Curve was generated by fitting the observed data to Eq. 4 using a unitary current of -0.43 pA at -50 mV. The slope of the line yielded an estimated P_o of 0.94.

This latter set of measurements was conducted within the first 60 s after cell swelling was initiated. As illustrated in Fig. 7, these three measurements of unitary conductance are in close agreement indicating that single-channel current does not change during activation.

Given that the unitary conductance of VSOAC is constant, we conclude that the assumption that macroscopic current increases by graded increases in P_o of a fixed number of channels is incorrect. The simplest hypothesis that would account for the

observed stationary noise analysis data is illustrated by the following kinetic scheme



where *C* is the closed channel, *O* is the open channel and *I* is the inactivated channel (see Jackson and Strange, 1995). In this scheme, activation of VSOAC is due to an abrupt switching of single channels from an OFF state ($P_o = 0$) to an ON state. In the ON state, channels switch between open and closed states and open and inactivated states.¹ The consequence of this model is that the swelling-induced increase in whole-cell current is due to an increase in the number of ON channels. In other words, the number of active channels in the membrane is not constant and P_o does not increase in a graded fashion.

Eq. 4 is derived from Eqs. 1 and 2 and expresses σ^2 in terms of a fixed P_o and a variable *N*

$$\sigma^2 = iI(1 - P_o). \tag{4}$$

The lower curve in Fig. 11 was obtained by fitting the observed stationary noise analysis data (*solid points*) with Eq. 4 and $i = -0.43$ pA as determined by single-channel measurements. The slope of this line yields an estimate of single-channel P_o of 0.94. For all five cells on which stationary noise analysis was performed, the mean \pm SE P_o estimated using Eq. 4 was 0.94 ± 0.01 , a value in close agreement with our single-channel measurements (see also Solc and Wine, 1991; Okada et al., 1994). We conclude that swelling-induced activation of VSOAC involves an abrupt switching of single channels from the OFF state where $P_o = 0$ to the ON state where P_o is close to unity.

Spectral Analysis

In addition to confirming the adequacy of the recording bandwidth, spectral analysis also provides information on channel gating kinetics. For a channel that switches between an open and a closed state



the relaxation time constant τ is given by

$$\tau = 1/(k_1 + k_{-1}) \tag{5}$$

The relaxation time constant is related to the measured corner frequency f_c of the spectral data by

$$\tau = 1/2 \pi f_c. \tag{6}$$

At low channel P_o where k_1 is very small, τ approximates $1/k_{-1}$, which is the

¹ Transition of the channel into the inactivated state is only observed during strong depolarization (see Jackson and Strange, 1995).

mean-channel open time. Conversely, if channel P_o is very high, τ approximates $1/k_1$, which is the mean-channel closed time. Given our conclusion that cell swelling switches individual VSOAC channels from an OFF state abruptly to an ON state with a P_o near unity, the mean f_c of 526 Hz gives an estimated mean-channel closed time of 0.3 ms.

Speculation on the Nature of VSOAC

We have argued previously that the main function of VSOAC is to transport small organic solutes across the cell membrane in a relatively nonselective manner (Jackson et al., 1994; Strange and Jackson, 1995). In this regard, it is noteworthy that the brief, spontaneous closures and high, apparently fixed P_o of VSOAC are characteristic of porins, a primitive class of channels that function largely to transport organic solutes nonselectively across bacterial outer membranes (Benz, 1988; Benz and Bauer, 1988; Berrier, Coulombe, Houssin, and Ghazi, 1992, 1993). The physiological role and electrophysiological properties of VSOAC suggest indirectly that it may be a "porin-like" channel.

The porin-like characteristics of VSOAC call attention to recent studies on the protein I_{Cln} (Paulmichl, Wickman, Ackerman, Peralta, and Clapham, 1992; Abe, Takeuchi, Ishii, and Abe, 1993; Krapivinsky, Ackerman, Gordon, Krapivinsky, and Clapham, 1994). When overexpressed in *Xenopus* oocytes, I_{Cln} gives rise to a constitutively active anion current with characteristics identical to those of VSOAC (Paulmichl et al., 1992; Abe et al., 1993; Paulmichl, Gschwentner, Wöll, Schmarada, Ritter, Kanin, Ellemunter, Waitz, and Deetjen, 1993). In addition, I_{Cln} antisense oligonucleotides and a monoclonal anti- I_{Cln} antibody inhibit the outwardly rectified, swelling-activated anion currents in NIH 3T3 cells (Gschwentner, Nagl, Wöll, Schmarada, Ritter, and Paulmichl, 1995) and *Xenopus* oocytes (Ackerman et al., 1994, respectively). Structural analysis suggests that the I_{Cln} protein forms four β strands but no transmembrane helices (Paulmichl et al., 1992). Based on these findings, Paulmichl et al. (1992) proposed that I_{Cln} codes for a novel anion channel with a pore region formed by an eight-stranded antiparallel β barrel.

More recently, Krapivinsky et al. (1994) demonstrated that I_{Cln} codes for an abundant, soluble, highly acidic protein located primarily in the cytoplasm. This protein forms tight oligomeric complexes with other cytoplasmic proteins including actin. These findings led Krapivinsky et al. (1994) to propose that I_{Cln} is not an anion channel, but a channel regulator. Overexpression of I_{Cln} in *Xenopus* oocytes was postulated to activate an endogenous volume-sensitive anion conductance (Ackerman et al., 1994).

Beta barrels are a defining structural characteristic of porins (Benz, 1988; Benz and Bauer, 1988; Rosenbusch, 1990). In addition, porins are soluble, highly acidic proteins that insert spontaneously into lipid bilayers and cell membranes (Pfaller, Freitag, Harmey, Benz, and Neupert, 1985; Benz, 1988; Benz and Bauer, 1988; Rosenbusch, 1990; Eisele and Rosenbusch, 1990). If I_{Cln} codes for an anion channel as suggested by Paulmichl et al. (1992), it is interesting to speculate that swelling-induced activation may involve release of the protein from a cytoplasmic binding site followed by spontaneous membrane insertion. The insertion of the protein into the cell membrane would account for the abrupt switching of single channels from an OFF to an ON state. Extensive additional studies are required to determine whether

I_{Clh} functions as an organic osmolyte/anion channel and to ascertain if channel activation is mediated by spontaneous membrane insertion events.

We thank Drs. Simon Lewis, Chris Miller, and Kari Nadeau for critically reviewing the manuscript, Dr. Bruce Bean for helpful and stimulating discussions, and Cambridge Neurosciences for technical assistance.

This work was supported by NIH grants NS30591 and DK45628. K. Strange is an Established Investigator of the American Heart Association. P. Jackson was supported by the Boston Neurosurgical Foundation and by NIH training grant T32EY07110.

Original version received 11 October 1994 and accepted version received 5 January 1995.

REFERENCES

- Abe, T., K. Takeuchi, K. Ishii, and K. Abe. 1993. Molecular cloning and expression of a rat cDNA encoding MDCK-type chloride channel. *Biochimica et Biophysica Acta*. 1173:353–356.
- Ackerman, M. J., K. D. Wickman, and D. E. Clapham. 1994. Hypotonicity activates a native chloride current in *Xenopus* oocytes. *Journal of General Physiology*. 103:153–179.
- Banderali, U., and G. Roy. 1992. Anion channels for amino acids in MDCK cells. *American Journal of Physiology*. 263:C1200–C1207.
- Benz, R. 1988. Structure and function of porins from gram-negative bacteria. *Annual Review of Microbiology*. 42:359–393.
- Benz, R., and K. Bauer. 1988. Permeation of hydrophilic molecules through the outer membrane of gram-negative bacteria. Review on bacterial porins. *European Journal of Biochemistry*. 176:1–19.
- Berrier, C., A. Coulombe, C. Houssin, and A. Ghazi. 1993. Voltage-dependent cationic channel of *Escherichia coli*. *Journal of Membrane Biology*. 133:119–127.
- Berrier, C., A. Coulombe, C. Houssin, and A. Ghazi. 1992. Fast and slow kinetics of porin channels from *Escherichia coli* reconstituted into giant liposomes and studied by patch-clamp. *Federation of European Biochemical Societies*. 306:251–256.
- Conti, F., B. Hille, and W. Nonner. 1984. Non-stationary fluctuations of the potassium conductance at the node of Ranvier of the frog. *Journal of Physiology*. 353:199–230.
- Doroshenko, P., and E. Neher. 1992. Volume-sensitive chloride conductance in bovine chromaffin cell membrane. *Journal of Physiology*. 449:197–218.
- Eisele, J.-L., and J. P. Rosenbusch. 1990. *In vitro* folding and oligomerization of a membrane protein. Transition of bacterial porin from a random coil to a native conformation. *Journal of Biological Chemistry*. 265:10217–10220.
- Garcia-Perez, A., and M. B. Burg. 1991. Renal medullary organic osmolytes. *Physiological Reviews*. 71:1081–1115.
- Gschwentner, M., U. O. Nagl, E. Wöll, A. Schmarda, M. Ritter, and M. Paulmichl. 1995. Antisense oligonucleotides suppress cell volume-induced activation of chloride channels. *Pflügers Archiv*. In Press.
- Hallows, K. R., and P. A. Knauf. 1994. Principles of cell volume regulation. In *Cellular and Molecular Physiology of Cell Volume Regulation*. K. Strange, editor. CRC Press, Boca Raton, FL. 3–29.
- Heinemann, S. H., and F. Conti. 1992. Nonstationary noise analysis and application to patch clamp recordings. *Methods in Enzymology*. 207:131–148.
- Hille, B. 1992. *Ionic Channels of Excitable Membranes*. Sunderland Associates, Inc., Sunderland, MA. 312 pp.
- Jackson, P. S., and K. Strange. 1993. Volume-sensitive anion channels mediate swelling-activated inositol and taurine efflux. *American Journal of Physiology*. 265:C1489–C1500.

- Jackson, P. S., and K. Strange. 1995. Characterization of the voltage-dependent properties of a volume-sensitive anion conductance. *Journal of General Physiology*. 105:661–677.
- Jackson, P., R. Morrison, and K. Strange. 1994. The volume-sensitive organic osmolyte-anion channel VSOAC is regulated by non-hydrolytic ATP binding. *American Journal of Physiology*. 267:C1203–C1209.
- Kirk, K., J. C. Ellory, J. D. Young. 1992. Transport of organic substrates via a volume-activated channel. *Journal of Biological Chemistry*. 267:23475–23478.
- Krapivinsky, G. B., M. J. Ackerman, E. A. Gordon, L. D. Krapivinsky, and D. E. Clapham. 1994. Molecular characterization of a swelling-induced chloride conductance regulatory protein, pI_{Cl^-} . *Cell*. 76:439–448.
- Lewis, R. S., P. E. Ross, and M. D. Cahalan. 1993. Chloride channels activated by osmotic stress in T lymphocytes. *Journal of General Physiology*. 101:801–826.
- McManus, M., C. Serhan, P. Jackson, and K. Strange. 1994. Ketoconazole blocks organic osmolyte efflux independent of its effect on arachidonic acid conversion. *American Journal of Physiology*. 267:C266–C271.
- Nilius, B., M. Oike, I. Zahradnik, and G. Droogmans. 1994. Activation of a Cl^- current by hypotonic volume increase in human endothelial cells. *Journal of General Physiology*. 103:787–805.
- Okada, Y., C. C. H. Petersen, M. Kubo, S. Morishima, and M. Tominaga. 1994. Osmotic swelling activates intermediate-conductance Cl^- channels in human intestinal epithelial cells. *Japanese Journal of Physiology*. 44:403–409.
- Paulmichl, M., M. Gschwenter, E. Wöll, A. Schmarla, M. Ritter, G. Kanin, H. Ellemunter, W. Waitz, and P. Deetjen. 1993. Insight into the structure-function relation of chloride channels. *Cellular Physiology and Biochemistry*. 3:374–387.
- Paulmichl, M., Y. Li, K. Wickman, M. Ackerman, E. Peralta, and D. Clapham. 1992. New mammalian chloride channel identified by expression cloning. *Nature*. 356:238–241.
- Pfaller, R., H. Freitag, M. A. Harmey, R. Benz, and W. Neupert. 1985. A water-soluble form of porin from the mitochondrial outer membrane of *Neurospora crassa*. Properties and relationship to the biosynthetic precursor form. *Journal of Biological Chemistry*. 260:8188–8193.
- Rosenbusch, J. P. 1990. Structural and functional properties of porin channels in *E. coli* outer membranes. *Experientia*. 46:167–173.
- Sigworth, F. J. 1980. The variance of sodium current fluctuations at the node of Ranvier. *Journal of Physiology*. 307:97–129.
- Solc, C. K., and J. J. Wine. 1991. Swelling-induced and depolarization-induced Cl^- channels in normal and cystic fibrosis epithelial cells. *American Journal of Physiology*. 261:C658–C674.
- Stoddard, J. S., J. H. Steinbach, and L. Simchowicz. 1993. Whole cell Cl^- currents in human neutrophils induced by cell swelling. *American Journal of Physiology*. 265:C156–C165.
- Strange, K. 1994. Are all cell volume changes the same? *News in Physiological Sciences*. 9:223–228.
- Strange, K., and P. S. Jackson. 1995. Swelling-activated organic osmolyte efflux: a new role for anion channels. *Kidney International*. In press.
- Strange, K., K. Churchwell, N. Ballatori, J. L. Boyer, and P. S. Jackson. 1995. Properties of volume-sensitive organic osmolyte/anion channels (VSOAC) in hepatocytes of the marine skate *Raja erinacea*. *Federation of American Societies of Experimental Biology Journal*. 9:A636. (Abstr.)
- Worrell, R. T., A. G. Butt, W. H. Cliff, and R. A. Frizzell. 1989. A volume-sensitive chloride conductance in human colonic cell line T84. *American Journal of Physiology*. 256:C1111–C1119.
- Wunder, U. R., and M. Colombini. 1991. Patch clamping VDAC in liposomes containing whole mitochondrial membranes. *Journal of Membrane Biology*. 123:83–91.
- Yancey, P. H. 1994. Compatible and counteracting solutes. In *Cellular and Molecular Physiology of Cell Volume Regulation*. K. Strange, editor. CRC Press, Boca Raton, FL. 81–109.